



**HAL**  
open science

# Full-Wave simulations of the enhanced Upper-Hybrid Resonance Scattering

Stéphane Heuraux, O Krutkin, E Gusakov, F da Silva

► **To cite this version:**

Stéphane Heuraux, O Krutkin, E Gusakov, F da Silva. Full-Wave simulations of the enhanced Upper-Hybrid Resonance Scattering. IRW 14th Lausanne, Suisse 22-24th May 2019, May 2019, Lausanne, Switzerland. hal-02963094

**HAL Id: hal-02963094**

**<https://hal.univ-lorraine.fr/hal-02963094>**

Submitted on 9 Oct 2020

**HAL** is a multi-disciplinary open access archive for the deposit and dissemination of scientific research documents, whether they are published or not. The documents may come from teaching and research institutions in France or abroad, or from public or private research centers.

L'archive ouverte pluridisciplinaire **HAL**, est destinée au dépôt et à la diffusion de documents scientifiques de niveau recherche, publiés ou non, émanant des établissements d'enseignement et de recherche français ou étrangers, des laboratoires publics ou privés.

## Full-Wave simulations of the enhanced Upper-Hybrid Resonance Scattering

S. Heuraux<sup>1</sup>, O. Krutkin<sup>1,2</sup>, E. Gusakov<sup>2</sup>, F. da Silva<sup>3</sup>

<sup>1</sup>*Institut Jean Lamour, CNRS-Université de Lorraine, BP 50840, F-54011 Nancy, France*

<sup>2</sup>*Ioffé Institut S' Peterburg, Russia Federation*

<sup>3</sup>*Instituto de Plasmas e Fusão Nuclear, Instituto Superior Técnico, Av. Rovisco Pais, n°1, Lisbon, Portugal*

### Introduction:

The aim of this work is to improve the simple linear interpretative model usually applied to extract turbulence characteristics of tokamak plasmas using data of Upper-Hybrid Resonant Scattering (UHRS) experiments [1]. To evaluate the limits of such model, full-wave simulations have to be performed. These computations are complex due to the fact that the spatial scales change a lot especially as the wave propagates in vicinity of the resonance. Close to the resonance the mode conversion should be taken into account, which requires considering both components of the wave electric field together with the thermal effects. The amplitude of the electromagnetic component  $E_y$ , remains finite overall the propagative zone, which can be used in computational scheme. However the group velocity decreases drastically and can reach in principle a velocity close to zero as it was shown numerically [2] and experimentally [3-4]. This cold plasma approximation is inapplicable for our problem, and the thermal effects have to be included to describe the wave conversion from extraordinary mode (X-mode) to a warm plasma mode as mentioned in [1]. However the possible mode conversion described by the warm plasma model used corresponds to a warm wave propagating in an opposite direction to the one expected in tokamaks for the probing frequency close to the fundamental electron cyclotron harmonic due to constraints of the numerical scheme. Assuming that the probing wave propagates along the resonance cone which assumes to have a parallel wavenumber, ignored here, giving more or less a propagation at constant density, so 1D-studies on the Doppler shift induced by moving structures near the resonance were performed to evaluate if the effective Doppler shift obtained is directly connected to the velocity of the scattering structure. The scattering efficiency above the limitations of the [1] model is also provided for different cases. To finish an estimation of the parameters required to simulate realistic cases is provided and corresponds to the existing devices such as FT2, WEST, and what could be expected from the full-wave simulation to interpret more accurately the UHRS diagnostic measurements.

### Back to basics:

The assumptions for the X-mode including slow time evolution of the plasma parameters and the writing of the time-dependent wave equation can be found in [5]. This set of partial differential equations in one-dimension in space can be reduced to:

$$\begin{cases} \partial_t^2 E_x + \omega_p^2 E_x = \omega_p^2 v_y \\ \partial_t^2 E_y - c^2 \partial_x^2 E_y + \omega_p^2 E_y = \omega_p^2 v_x \\ \partial_t v_y = -\omega_c E_y + \omega_c v_x \\ \partial_t v_x = -\omega_c E_x - \omega_c v_y \end{cases}$$

The numerical scheme including variable normalizations used to compute the electric field components is described in [6]. To save computing time to reach the vicinity of the upper-hybrid resonance, it is better to use a steady state configuration in the monochromatic case which permits to reduce, in the 1-D case, to an Helmholtz equations where the X-mode is used to compute y-component of the electric field and a polarization equation is used to deduce x-component of the wave electric field. The advantage is that  $E_y$  component stays finite without collision. The question in this case is if the scattering is fully and correctly described? The index of X-mode for a given probing pulsation  $\omega$  follows the expression:

$$N_x^2 = 1 - \frac{\omega_{pe}^2 (\omega^2 - \omega_{pe}^2)}{\omega^2 (\omega^2 - \omega_{ce}^2 - \omega_{pe}^2)}$$

where  $\omega_{pe}$  is the electron plasma pulsation and  $\omega_{ce}$  electron cyclotron pulsation. In a tokamak the way to reach the resonance is to launch the probing wave from the high field side fulfilling the condition  $\omega > \omega_{ce\_min}$  ( $\omega_{ce}$  at the low field side),  $\omega < \omega_{ce\_max}$  and  $\omega > \omega_{L\_max}$  (left circular cut-off pulsation or  $f_c$ .) for high density plasma  $\omega_{pe} \gg \omega_{ce}$ .

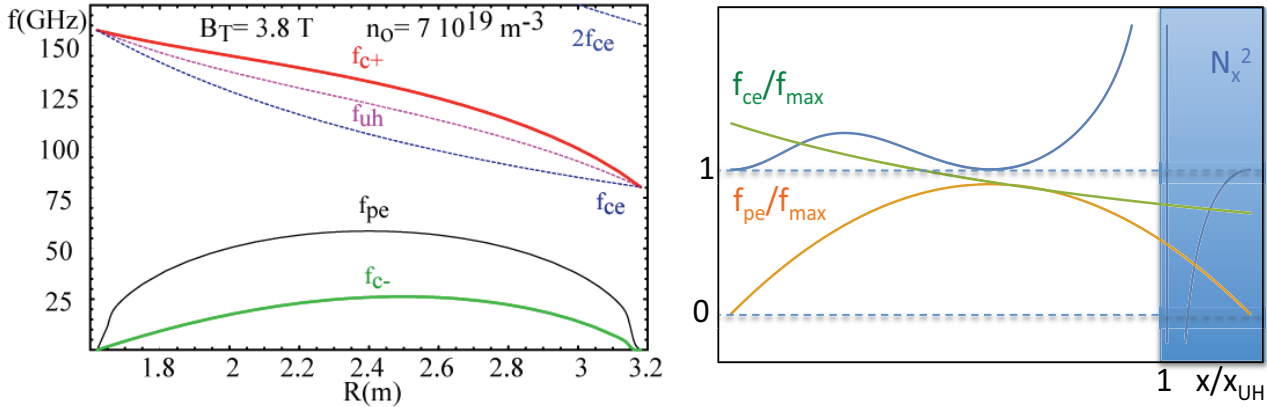


Figure 1: Density and magnetic field intensity profiles of standard Tore Supra discharges and associated cut-offs and resonance frequencies (left) and (right) X-mode index square with plasma and electron cyclotron normalized frequencies versus position normalized by  $x_{UH}$  upper-hybrid resonance position for a probing frequency of 90 GHz.

For the warm plasma description, the pressure term is added to the electron fluid equation as following:

$$\partial_t \vec{v} = -\frac{e}{m_e} \vec{E} - \frac{e}{m_e} \vec{v} \times \vec{B} - \frac{k_B T_e}{m_e n_e(x)} \vec{\nabla} P_e$$

This equation is combined with Maxwell's equations using the same normalization as before. The time-dependent set of differential equations for X-mode in the warm plasma approximation is written as:

$$\left\{ \begin{array}{l} \partial_t^2 E_x - v_{Te}^2 \partial_x^2 E_x + \omega_{pe}^2 E_x = -\omega_{pe}^2 v_y \\ \partial_t^2 E_y - c^2 \partial_x^2 E_y + \omega_{pe}^2 E_y = \omega_{pe}^2 v_x \\ \partial_t v_x = -\omega_{ce} (1 + \lambda_{De}^2 \partial_x^2) E_x - \omega_{ce} v_y \\ \partial_t v_y = -\omega_{ce} E_y + \omega_{ce} v_x \end{array} \right.$$

where  $\lambda_{De}$  is the Debye length and  $v_{Te}$  is the electron thermal velocity. This system is solved numerically using for the 1<sup>st</sup> equation a Numerov method of 4<sup>th</sup> order in time where  $v_{Te}^2 \partial_x^2 E_x$  is treated as a source term and can be evaluated at the wanted order in space, for the 2<sup>nd</sup> wave equation Colin's scheme [6] at the 2<sup>nd</sup> order in time and space using magic step, for the last equations of the motion a Runge-Kutta (RK45) scheme where  $v_{Te}^2 \partial_x^2 E_x$  is evaluated from the first equation. These numerical methods are associated to transparent boundary conditions at the mesh border, which are different for the electromagnetic wave and for the electron acoustic wave equations. The use of UTS (Unidirectional Transparent Source) [7] permits a direct access to the scattered wave. This code permits to determine numerically the position where the mode conversion can occur, and, thus thanks to monotonous increase of the probing wave wavenumber with the radial coordinate, deduce the wavenumber cut above which the higher wavenumber can be ignored in the interpretation model of the UHRS data.

### Results on the UHRS efficiency:

To evaluate the UHRS efficiency as function of density fluctuation wave number, computations have been done for a given plasma density and magnetic field intensity profiles in cold approximation with artificially introduced damping factor near UHR. However using a Helmholtz equation we need to determine the insensibility modulation in vacuum making it impossible to reduce the computation time by squeezing part of the plasma, launching the wave into the plasma and looking at the vicinity of the resonance. But as the phase measurement is not an issue to determine the scattered power, it is possible to compress the range of radius without contribution. This compression, however, imposes some limitations. If the index gradient is too high some spurious reflection can be generated. The density profile and magnetic field must be compressed in the same way up to a smooth transition to the radius range of interest where no compression exists. An hyperbolic tangente transition function is used to ensure that no spurious reflection occurs. To avoid misinterpretations no density fluctuation is put in this area. As consequences the range of fluctuation wavenumbers is limited to values above  $2 k_0$  where  $k_0$  is the vacuum wavenumber. To approach the resonance close enough, the number of points per wavelength in vacuum is of the order of 10000 points per vacuum wavelength. At the same time the damping factor has to be optimized to damp the wave without generating spurious reflection. The last keypoint is not easy to fulfil. Most of the time a residual reflection imposes restriction on the scattered power detectable here  $P_s/P_0 \sim 10^{-3}$ . This reduces the range of density fluctuation parameters in which the linear behaviour can be studied. Taking into account these constraints the UHRS efficiency was studied for the standard Tore Supra case requiring 84000 grid points. To improve the accuracy even more, more points are needed but the computing time would become too large since a minimum of 30 wavenumber values is needed to elaborate a curve for one value of the density fluctuations. Another important point is the shape of the envelop used to study this efficiency, such as a Gaussian shape or a wavetrain covering all the plasma. The wavetrain has the advantage to have an unique wavenumber value but in this case the harmonic of the Bragg rule should be taken into account for the interpretation[8]. The Gaussian shape localizes more the scattering process but the wavenumber spectrum has a finite width.

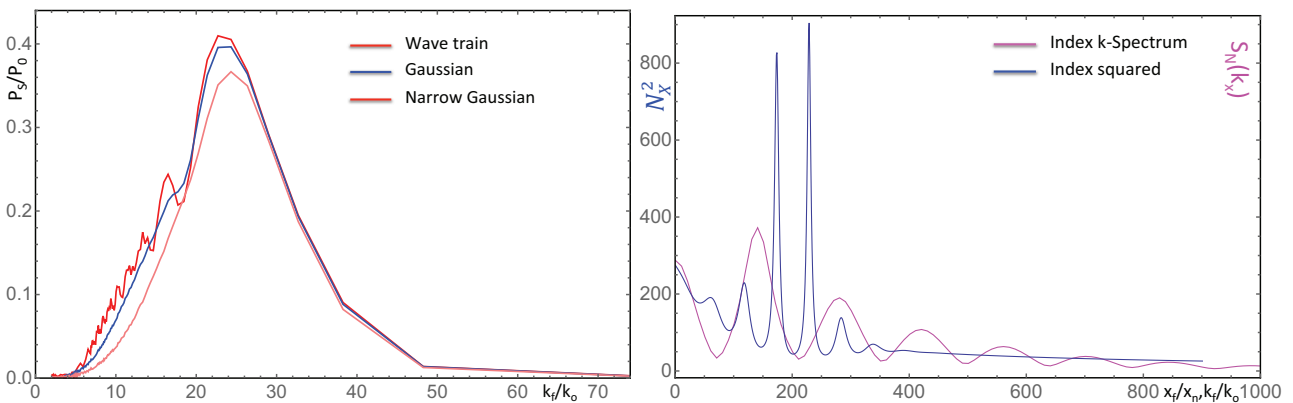


Figure 2: UHRS efficiency as function of fluctuation wavenumber normalized to vacuum wave number for three envelop shapes (left) and local index squared variations (Gaussian shape for the density perturbation) and associated index k-spectrum in the vicinity of the resonance as function of normalized coordinates (right).

The impact of the shape is clearly seen on Fig. 2 where the interferences (modulation of the efficiency) of scattered waves are present, except for the case of a narrow Gaussian shape. Nevertheless for the Gaussian shape there is a contribution at the low wavenumber values. The decay at high  $k$ -values is due to the damping introduced to ensure the wave absorption in the close vicinity of UHR. If instead of the density perturbations an index modulation is used, the behaviour of the efficiency changes drastically due to the fact that the index k-spectrum is more well defined, however the width of the Gaussian covers a large range of the unperturbed index values. This fact gives a rather flat variation of the high wavenumber efficiency around the vicinity of the UHR.

### Mode conversion X-mode to electrom warm plasma mode:

A previous article [9] shown the possibility to describe the wave propagation in warm plasma approximation in the time-domain without using Particle In Cell code. Here we have used a gradient pressure perturbation corresponding to the linear perturbation induced by the probing wave. The goal of such computation is to determine, in a time-dependent problem, the k-value for which the mode conversion occurs. The evaluation of the scattered power should take of the mode conversion power for the wavenumber values above this k-value, which means a reduction of the Bragg backscattering efficiency on the X-mode above the conversion point. As shown in [1] knowing the k-range becomes and the efficiency, permits to interpret the frequency spectrum obtained by a UHRS diagnostic on WEST the upgrade of Tore Supra tokamak [10]. On Figure 3, the  $E_x$  component exhibits two typical wavelengths, the longest one is linked to X-mode, and the shortest wavelength is identified as the warm mode. The warm mode group velocity is then connected to the electron thermal velocity, which propagates slowly than the X-mode except when the X-mode wave approaches the resonance where both propagates more or less at the same speed. Unlike the X-mode the warm wave can cross the resonance without change, and carry the wave energy outside the resonance zone. The conversion X-mode to warm mode is forward conversion. The direct backward conversion cannot be computed due to the fact the scheme is numerical instable for backward warm mode. The tests performed do not show any influence on Bragg rules by a possible coupling to the warm mode. This tool is able to describe the mode conversion from X-mode and warm in time-dependent description, and can be used to studied the effects of the density fluctuations on this process in a dynamic way as it was done in the cold plasma plasma approximation to explain why the frequency spectrum is so large. However it is clear that an accurate electron temperature is required to apply such tools for the UHRS data interpretation.

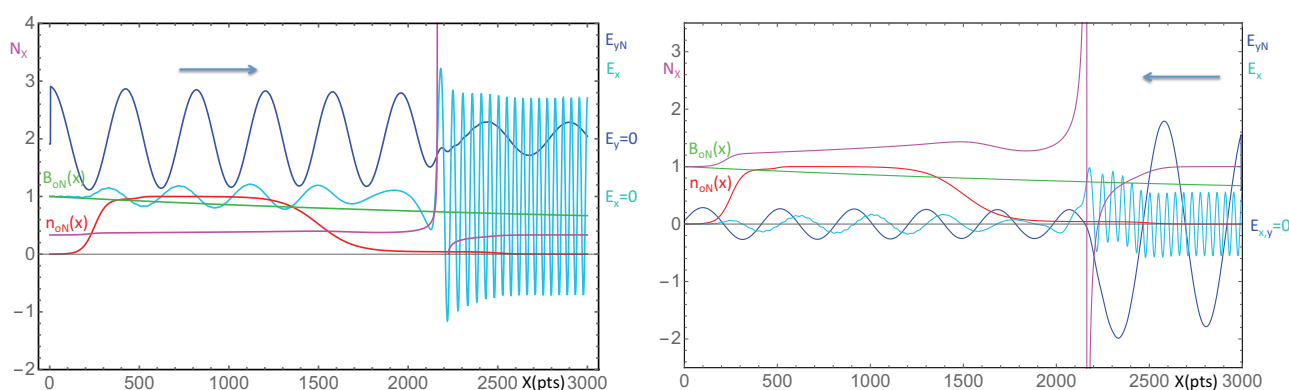


Figure 3: X-mode (lower branch) Warm mode conversion (right) and X-mode (upper branch) to Warm mode conversion (left) for the same plasma and wave parameter profiles.

### Conclusion:

The efficiency of the Bragg backscattering was obtained for relevant tokamak plasma parameters. Depending on the envelop of density fluctuations used to evaluate this efficiency, different contributions appear at low k-values. The upper bound of the integration in collisionless plasma can be accessed determining at the position of the conversion X to Warm mode using the code XtoW.

### Bibliography:

- [1] K.M. Novik, A.D. Piliya Plasma Phys. Control. Fusion **35** (1993) 357-381.
- [2] B. Brusehaber, E. Gusakov, Kramer M., A. Piliya Plasma Physics and Control. Fusion, **36** (1994) 997-1012
- [3] V.I. Arkhipenko, V. Brusehaber, V. Budnikov et al. Plasma Phys. and Control. Fus., **37A** (1995) 347-358.
- [4] D.G. Bulyginiskiy, A.D. Gurchenko, E.Z. Gusakov et al. Physics of Plasmas, **8** (2001) 2224.
- [5] S. Heurax, F. da Silva Aims Journal Discrete&Continuous Dynamical Systems - Series S **5** (2012) 307-328.
- [6] M. Colin PhD thesis, University of Lorraine 2001.
- [7] F. da Silva, S. Heurax, S. Hacquin, M. Manso J. Comp. Phys **203** (2005) 467-492.
- [8] I. Boucher *et al* Plasma Phys. Control. Fusion **40** (1998) 1489-1500.
- [9] W. Tierens, D. De Zutter Phys of Plasmas **19** (2012) 112110.
- [10] C. Bourdelle *et al.* WEST Physics Basis. Nuclear Fusion **55** (2015) 063017.